# Analytical formulation of the elastic-plastic behaviour of bi-symmetrical steel shapes

António Manuel Baptista[a,]*, Jean-Pierre Muzeau[b]

[a]*Dep. Estruturas, LNEC, av. do Brasil 101, 1700-066 Lisboa Codex, Portugal*
[b]*LGC, CUST, Blaise Pascal University, BP 206, 63174 Aubière Cedex, France*

**Abstract**

This paper presents the analytical relationships of a non-linear model for the in-plane elastic-plastic analysis of bi-symmetrical steel shapes bent about one of their main axes. The basic variables are the cross-section global deformations from which it is possible to evaluate the internal loads and the cross-section stiffness matrix components by means of simple expressions. Furthermore, the values of stresses and strains at any point of the cross-section may be determined knowing the values of the internal loads, in the elastic and elastic-plastic domains. The effects of progressive yielding spreading, as well as those of material strain-hardening, are taken into account in the evaluation of the cross-section resistance capacity in the elastic-plastic domain. This analytical model represents an efficient, simple and accurate alternative to the elastic-plastic models based on numerical methods.

*Keywords:* Analytical model; Elastic-plastic behaviour; Cross-section; Global deformation interaction; Internal forces interaction; Strain-hardening; Resistance capacity; Deformation capacity; Stiffness

---

* Corresponding author: Tel.: +351 21 844 3252; fax: +351 21 844 3025;
E-mail address: ambaptista@lnec.pt

# 1. Introduction

Before reaching their ultimate limit states, most of steel structures present non-linear behaviours. Therefore, an accurate analysis of such structures must take into account the most important factors related to these non-linearities. More, a realistic simulation of the elastic-plastic behaviour should allow the effects of the yielding spreading inside the cross-sections to be taken into account.

Usually, this type of analysis is carried out by means of numerical models, most of them being based on the finite element method, associated to a more or less fine meshing of the cross-sections into fibres or layers. Internal forces and stiffness matrix components are obtained by numerical integration, over the whole cross-section, of the average stress and stiffness of each elementary area, fibre or layer. However, this type of calculation is very heavy, and it requires a large number of data to be recorded during the iterations of the non-linear calculations.

Otherwise, the elastic-plastic analysis may be carried out by means of analytical cross-section models. These models are usually based on $N-M$ interaction curves under the hypothesis of perfect elastic-plastic behaviour, without strain hardening.

They are often written under the form:

$$\left(\frac{N}{N_p}\right)^{\alpha}+\left(\frac{M}{M_p}\right)^{\beta}\leq 1. \tag{1}$$

Although this type of expression is very common in practice, it presents several limitations regarding the actual material behaviour [1]. This paper presents an analytical formulation for the in-plane analysis of the elastic-plastic behaviour of bi-symmetrical

cross-sections made of orthogonal rectangular elements (I-shaped cross-sections or rectangular hollow sections, for instance) in the case of bending about the strong or weak axis.

The general theoretical principles of this formulation are presented in [2,3,4]. The basic variables are the cross-section global deformations, from which it is possible to evaluate the internal loads and the cross-section stiffness matrix components, by means of simple mathematical expressions. These expressions cover all the possible combinations of deformation states in the elastic-plastic domain: yielding (in tension or compression) of one or two tips of the flanges, partial yielding of the section web, and total yielding of the cross-section.

The model allows the yielding spreading across the sections to be taken into account as well as the effects of the strain hardening on their resistance capacity. The bending/axial deformation interaction effects are considered and the cross section resistance may be limited by the deformation capacity of the material or, in other words, by its ductility. This characteristic allows the control of the cross-section ultimate limit states associated to this material property.

This model represents an efficient, simple and accurate alternative to the elastic-plastic methods of analysis based on the numerical integration of stresses and stiffness over the cross-section. It may be useful to check some design requirements specified in modern Standards for the design of steel structures, such as Eurocode 3 [5] for instance.

In section “5.4 - Methods of analysis considering material non-linearities”, the EN 1993-1-1 Standard [5] allows the “non-linear plastic analysis considering the partial plastification of members in plastic zones”. It gives also some conditions for the use of plastic global analysis of steel structures, such as capacity of the members for sufficient

rotation or the stability of members at plastic hinges, which may be checked using this model. The analytical formulation explained in this paper establishes a relationship between the internal forces and the global deformations of the cross-sections, taking in account their geometric proportions and the effects of material hardening. Therefore, it allows a good evaluation of the structural members' deformations and displacements, either in the elastic or elastic-plastic domains of behaviour, and, consequently, a better estimation of the stiffness and deformed geometry of the structure, that control its stability and serviceability limit states.

## 2. Basic principles of the non-linear mechanical model

The evolution of the cross-section non-linear behaviour depends only on "behaviour factors" associated to its shape or to the constitutive law of its material.

The evaluation of the internal forces and stiffness matrix components depend on these "behaviour factors" and on "scale factors", such as the elastic modulus $E$, the yield stress $\sigma_y$ or the dimensions of the cross-section, which allow the results to be expressed in a certain system of units.

A more detailed explanation about the distinction between these behaviour and scale factors is given in section 4.2.

The behaviour of the material is represented by a bilinear stress-strain constitutive law $\sigma = f(\varepsilon)$, identical for tension and compression (Fig. 1). The $\sigma(\varepsilon)$ path is always the same, for loading and unloading, which means that the effects of elastic discharges during an unloading process are not taken into account. However, these effects have been found to be negligible during most of the monotonic loading processes [2], if the

stress reversal amplitude is not very large. On the other hand, this model is not suitable for the analysis of a structure under cyclic loading, induced by a seismic action for instance. Another situation, where this hypothesis may easily affect the results, is during a structural buckling process in the elastic-plastic domain; in this case, the results given by this model will be usually conservative.

All loads and their corresponding effects are limited to the plan of the structure. The behaviour of the structural elements depends only on the strains normal to their cross-sections. Each cross-section is bi-symmetrical regarding its two main axes, denoted *u* and *v*; the axis *u* is always the bending axis, whether it is the strong or the weak axis (Fig. 2).

The distribution of the cross-section strains is based on the Bernoulli's hypothesis that the cross-sections remain plane after deformation, in the elastic and in the elastic-plastic domains (Fig. 2):

$$\varepsilon(v) = \varepsilon_N - \chi\, v \tag{2}$$

The analytical expressions for the evaluation of the cross-section internal loads and stiffness matrix components are written as a function of reduced (non dimensional) variables, obtained from the division of the model variables by suitable scale factors:

$$\xi = \frac{\varepsilon}{\varepsilon_y}\ ;\ \varsigma = \frac{\sigma}{E\ \varepsilon_y}\ ;\ \tau = \frac{v}{v_M}\ ;\ \eta = \frac{\varepsilon_N}{\varepsilon_y}\ ;\ \mu = \frac{v_M}{\varepsilon_y}\chi\ ;\ \gamma = \frac{E - E_t}{E} \tag{3}$$

where $E_t$ is the tangent modulus of the material, $\varepsilon_y = \sigma_y / E$ is the yield strain, $v_M$ is the largest distance of the extreme fibres to the cross-section centroid along the *v* axis, $\xi$ is the reduced strain, $\varsigma$ is the reduced stress, $\tau$ is the reduced *v* co-ordinate, $\eta$ is the reduced axial deformation and $\mu$ is the reduced curvature.

In the space of the global deformations ($\mu$, $\eta$), Eq. (2) may be written under the form of Eq. (4), which represents a straight line containing all the combinations of the global deformations ($\mu$, $\eta$) that induce a reduced strain $\xi(\tau)$ in a cross-section elementary fibre with a $\tau$ co-ordinate.

$$\xi(\tau) = \eta - \tau \mu . \tag{4}$$

Fig. 3 shows an example of the set of parallel straight lines, with a slope $\tau^s = +1$, containing the global deformations ($\mu$, $\eta$) leading to upper fibre strains $\xi^s$ (Fig. 2) equal to the limits ${}_u\xi$, ${}_y\xi$, $\xi_y$ and $\xi_u$ between the domains of linear stress evolution (Fig. 1): elastic-plastic in compression (from ${}_u\xi$ to ${}_y\xi$), elastic (from ${}_y\xi$ to $\xi_y$), and elastic-plastic in tension (from $\xi_y$ to $\xi_u$). These parallel straight lines bound three $\omega$ deformation domains (Fig. 3) in which the stress evolution of the upper fibre is always of the same type: elastic-plastic in tension $\omega^s_{ep}$, elastic $\omega^s_{el}$, or elastic-plastic in compression ${}_{ep}\omega^s$.

The intersection between the $\omega$ domains shown on Fig. 3 with those corresponding to the lower fibre of the section (where the $\tau^i$ slope is equal to -1), is represented on Fig. 4.

In the case of cross-sections without any shape discontinuities (rectangular or circular solid cross-sections for instance), the elementary zones defined by this intersection represent all the possible $\Omega$ domains of evolution of the global deformations $\eta$ and $\mu$, corresponding to all the possible combinations of elastic and yielded areas, in tension or compression, in the cross-section. Within each $\Omega$ domain,

the $\xi$ strains at the extreme fibres are always in the same $\omega$ domain. The $\sigma = f(\varepsilon)$ relationship being constant for each extreme fibre in each $\omega$ domain, it is possible to get analytical expressions for the calculation of the cross-section internal forces and stiffness matrix components, which are unique within each $\Omega$ domain [2].

For cross-sections with discontinuous shapes (I, H or hollow shapes), the analytical integration of stresses in the section is obviously affected by these discontinuities. So, it is necessary to add to the diagram of Fig. 4, the parallel straight lines representing the limits of the $\omega$ domains of the fibres at these discontinuities (web-flange discontinuities for instance).

Fig. 5 shows the additional parallel straight lines corresponding to the shape discontinuities in I-shape cross-sections. In this case, it is necessary to add two sets of straight lines, corresponding to the discontinuities between each flange and the web.

In the case of symmetrical cross-sections to both main axes of inertia, made of a material with a symmetrical behaviour in tension and compression, the domains of evolution of the global deformations (Fig. 5) are symmetrical to both axes $\eta$ and $\mu$, [2,3,4]. Therefore, only the first quadrant domains from Fig. 5, corresponding to the positive global deformations, need to be taken in account in the formulation of the cross-section behaviour. Therefore, the number of $\Omega$ domains shown on this figure may be reduced from 27 to 9. Fig. 6 represents these 9 domains and their numbering, in order to make their identification easier.

In the other domains, the calculation of the internal loads and stiffness matrix components may be achieved with the absolute values of $\eta$ and $\mu$, the right sign being

attributed to the results according to the real signs of $\eta$ and $\mu$. An example of application will be presented later to show this procedure.

## 3. Formulation of the analytical model

The analytical formulation of the cross-section internal forces and stiffness matrix components is carried out in a system of reduced variables. The reduced axial load $n$ and bending moment $m$ are expressed by Eqs. (5)-(6).

$$n = \frac{N}{N_y} \quad , \quad N_y = E\, A\, \varepsilon_y \,; \tag{5}$$

$$m = \frac{M}{M_y} \quad , \quad M_y = E\, I\, \chi_y \quad , \quad \chi_y = \frac{\varepsilon_y}{v_M} \,. \tag{6}$$

The expressions relating the components of the tangent stiffness matrix [$H$], Eq. (7), with those of the reduced stiffness matrix [$h$], Eq. (8), are defined by Eqs. (9a)-(9d).

$$\begin{Bmatrix} dN \\ dM \end{Bmatrix} = \begin{bmatrix} H_{11} & H_{12} \\ H_{21} & H_{22} \end{bmatrix} \begin{Bmatrix} d\,\varepsilon_N \\ d\chi \end{Bmatrix} . \tag{7}$$

$$\begin{Bmatrix} dn \\ dm \end{Bmatrix} = \begin{bmatrix} h_{11} & h_{12} \\ h_{21} & h_{22} \end{bmatrix} \begin{Bmatrix} d\eta \\ d\mu \end{Bmatrix} . \tag{8}$$

$$H_{11} = \frac{\partial N}{\partial n} \frac{\partial \eta}{\partial\, \varepsilon_N} h_{11} = EA\, h_{11} , \tag{9a}$$

$$H_{12} = \frac{\partial N}{\partial n} \frac{\partial \mu}{\partial \chi} h_{12} = E\, A\, v_M\, h_{12} \,, \tag{9b}$$

$$H_{21} = \frac{\partial M}{\partial m} \frac{\partial \eta}{\partial\, \varepsilon_N} h_{21} = E \frac{I}{v_M} h_{21} , \tag{9c}$$

$$H_{22} = \frac{\partial M}{\partial m}\frac{\partial \mu}{\partial \chi} h_{22} = EI\, h_{22}\,. \tag{9d}$$

The cross-section geometry may be characterised by the following reduced parameters:

$$\alpha_b = \frac{b''}{b'}\,, \tag{10}$$

$$\alpha_h = \frac{h''}{h'}\,. \tag{11}$$

The dimensions *h'*, *h''*, *b'* and *b''* are defined in Fig. 7 for I-shapes bent about their strong or weak axis and for rectangular hollow sections. When bending occurs over its strong axis, the shape is denoted I-shape. When it is bent about its weak axis, it is denoted H-shape. Any type of these cross-sections may be obtained by the addition or the subtraction of two rectangles, *R'* (*b'*×*h'*) and *R''* (*b''*×*h''*).

The area *A* of the steel cross-section is $A = A' + A''$, where $A' = b'\,h'$ and $A'' = -\,b''\,h''$, in the case of a hollow section or an I-shape, or $A' = b'\,h'$ and $A'' = b''\,h''$ in the case of a H-shape. Furthermore, the ratio *A'/A* may be expressed by:

$$\frac{A'}{A} = \frac{A'}{A' + A''} = \frac{1}{1 + A''/A'} = \frac{1}{1 + k_A}\,, \tag{12}$$

and the ratio *A''/A* by:

$$\frac{A''}{A} = \frac{A - A'}{A} = 1 - \frac{1}{1 + A''/A'} = 1 - \frac{1}{1 + k_A} = \frac{k_A}{1 + k_A} = k_A\,\frac{A'}{A}\,. \tag{13}$$

In the case of a hollow section or an I-shape $k_A = -\,\alpha_b\,\alpha_h$, and in the case of a H-shape $k_A = \alpha_b\,\alpha_h$.

The second moment of inertia, *I,* is $I = I' + I''$, where $I' = b' h'^3 / 12$ and $I'' = - b'' h''^3 / 12$, in the case of a hollow section or an I-shape, or $I' = b' h'^3 / 12$ and $I'' = b'' h''^3 / 12$ in the case a H-shape. Furthermore, the ratio *I′/I* may be expressed by:

$$\frac{I'}{I} = \frac{I'}{I' + I''} = \frac{1}{1 + I''/I'} = \frac{1}{1 + k_I}, \tag{14}$$

and the ratio *I″/I* by:

$$\frac{I''}{I} = \frac{I - I'}{I} = 1 - \frac{1}{1 + I''/I'} = 1 - \frac{1}{1 + k_I} = \frac{k_I}{1 + k_I} = k_I \frac{I'}{I}. \tag{15}$$

In the case of a hollow section or an I-shape $k_I = - \alpha_b \, \alpha_h^{\,3} = \alpha_h^{\,2} \, k_A$, and in the case of a H-shape $k_I = \alpha_b \, \alpha_h^{\,3} = \alpha_h^{\,2} \, k_A$.

The steel cross-section and the two rectangles, *R′* and *R″*, have the same centroid and they are submitted to the same strain distribution. So, the axial deformation $\varepsilon_N$ is the same for these three sections. Therefore, the reduced axial deformations $\eta'$ and $\eta''$ are equal to the reduced axial deformation $\eta$ of the steel cross-section.

The reduced curvature $\mu'$ of *R′* is equal to the reduced curvature of the steel cross-section $\mu$, since *h′* is equal to its height (measured along the axis *v*). On the other hand, the reduced curvature $\mu''$, calculated according to Eq. (2), is related to $\mu$ by the following relationship:

$$\mu'' = \frac{h''}{2} \frac{\chi}{\varepsilon_y} = \frac{h''}{2} \frac{2}{h'} \mu = \frac{h''}{h'} \mu = \alpha_h \, \mu. \tag{16}$$

According to the previous definitions expressed by Eqs. (5)-(9), and to the geometrical relationships given by Eqs. (10)-(15), the axial load, bending moment and stiffness matrix components may be calculated by the following expressions:

$$N = E\,A\,\varepsilon_y\;\; n = E\,A'\,\varepsilon_y\;\; n' \;+ E\,A''\,\varepsilon_y\;\; n'' = E\,A\,\varepsilon_y\;\; \frac{1}{1+k_A}\left(n' + k_A\; n''\right). \tag{17}$$

$$M = E\,I\,\chi_y\;\; m = E\,I'\,\chi_y{}'\; m' + E\,I''\,\chi_y{}''\; m'' = E\,I\,\chi_y\;\; \frac{1}{1+k_I}\left(m' + \frac{k_I}{\alpha_h}\, m''\right). \tag{18}$$

$$H_{11} = E\,A\;\; h_{11} = E\,A'\,h_{11}' + E\,A''\,h_{11}'' = E\,A\;\; \frac{1}{1+k_A}\left(h_{11}' + k_A\,h_{11}''\right), \tag{19a}$$

$$H_{12} = E\,A\;\; \frac{h'}{2}\; h_{12} = E\,A'\frac{h'}{2}\; h_{12}' + E\,A''\frac{h''}{2}\; h_{12}'' = \ldots$$

$$\ldots = E\,A\;\; \frac{h'}{2}\;\; \frac{1}{1+k_A}\left(h_{12}' + \alpha_h\; k_A\; h_{12}''\right), \tag{19b}$$

$$H_{21} = E\,I\;\; \frac{2}{h'}\; h_{21} = E\,I'\frac{2}{h'}\; h_{21}' + E\,I''\frac{2}{h''}\; h_{21}'' = \ldots$$

$$\ldots = E\,I\;\; \frac{2}{h'}\;\; \frac{1}{1+k_I}\left(h_{21}' + \frac{k_I}{\alpha_h}\, h_{21}''\right), \tag{19c}$$

$$H_{22} = E\,I\;\; h_{22} = E\,I'\,h_{22}' + E\,I''\,h_{22}'' = E\,I\;\; \frac{1}{1+k_I}\left(h_{22}' + k_I\; h_{22}''\right). \tag{19d}$$

The reduced internal forces ($n$ and $m$) and the stiffness matrix components ($h_{11}$, $h_{12}$, $h_{21}$ and $h_{22}$) of the two rectangles $R'$ and $R''$ may be evaluated by means of analytical expressions presented in [2]. These relationships represent the simplified version of a general analytical model developed for rectangular cross-sections made of a material with any constitutive law, approached by a multilinear function $\sigma = f(\varepsilon)$ [2].

From the former relationships (5)-(9), and the above mentioned analytical expressions, the calculation of the steel cross-section reduced internal forces and stiffness matrix components, for each $\Omega$ domain (Fig. 6), may be written according to Eqs. (20)-(53d). The limits of each $\Omega$ domain may be defined as a function of the strains at specific points (external and internal extreme fibres of the flanges (Fig. 5): $\xi^s = \eta - \mu$ ; $\xi^S = \eta - \alpha_h \, \mu$ ; $\xi^I = \eta + \alpha_h \, \mu$ ; $\xi^i = \eta + \mu$ . The symbol (**E**) indicates an elastic behaviour, (**T**) represents yielding in tension and (**C**) yielding in compression.

Domain ① (Fig. 8): $-1 \le \xi^s \le 1$ (**E**); $-1 \le \xi^S \le 1$ (**E**); $-1 \le \xi^I \le 1$ (**E**); $-1 \le \xi^i \le 1$ (**E**) (20)

Internal forces:

$$n = \eta \quad ; \quad m = \mu \, . \tag{21}$$

Stiffness matrix components:

$$h_{11} = h_{22} = 1 \quad ; \quad h_{12} = h_{21} = 0 \, . \tag{22}$$

Domain ② (Fig. 9): $-1 \le \xi^s \le 1$ (**E**); $-1 \le \xi^S \le 1$ (**E**); $-1 \le \xi^I \le 1$ (**E**); $\xi^i > 1$ (**T**) (23)

Internal forces:

$$n = \frac{1}{1 + k_A} \left( \eta - \frac{\gamma}{4 \mu} \left( \mu + \eta - 1 \right)^2 + k_A \, \eta \right) . \tag{24}$$

$$m = \frac{1}{1 + k_I} \left( \mu - \frac{\gamma}{4 \mu^2} \left( \mu + \eta - 1 \right)^2 \left( 2 \mu - \eta + 1 \right) + k_I \, \mu \right) . \tag{25}$$

Stiffness matrix components:

$$h_{11} = \frac{1}{1+k_A}\left(1-\frac{\gamma}{2\mu}(\mu+\eta-1)+k_A\right), \tag{26a}$$

$$h_{12} = -\frac{\gamma}{1+k_A}\frac{1}{4\mu^2}(\mu+\eta-1)(\mu-\eta+1), \tag{26b}$$

$$h_{21} = -\frac{\gamma}{1+k_I}\frac{3}{4\mu^2}(\mu+\eta-1)(\mu-\eta+1), \tag{26c}$$

$$h_{22} = \frac{1}{1+k_I}\left(1-\frac{\gamma}{2\mu}(\mu+\eta-1)\left(1-\frac{(\eta-1)(\mu-\eta+1)}{\mu^2}\right)+k_I\right). \tag{26d}$$

Domain ③ (Fig. 10): $\xi^s < -1$ (**C**); $-1 \le \xi^S \le 1$ (**E**); $-1 \le \xi^I \le 1$ (**E**); $\xi^i > 1$ (**T**) (27)

Internal forces:

$$n = \frac{1}{1+k_A}\left(\eta-\gamma\frac{\eta}{\mu}(\mu-1)+k_A\ \eta\right). \tag{28}$$

$$m = \frac{1}{1+k_I}\left(\mu-\gamma\left(\mu-\frac{3}{2}+\frac{3\eta^2+1}{2\mu^2}\right)+k_I\,\mu\right). \tag{29}$$

Stiffness matrix components:

$$h_{11} = \frac{1}{1+k_A}\left(1-\frac{\gamma}{\mu}(\mu-1)+k_A\right), \tag{30a}$$

$$h_{12} = -\frac{\gamma}{1+k_A}\frac{\eta}{\mu^2}, \tag{30b}$$

$$h_{21} = -\frac{\gamma}{1+k_I}\frac{3\eta}{\mu^2}, \tag{30c}$$

$$h_{22} = \frac{1}{1+k_I}\left(1-\gamma\left(1-\frac{3\eta^2+1}{\mu^3}\right)+k_I\right), \tag{30d}$$

Domain ④ (Fig. 11): $\xi^s \geq 1$ (**T**); $\xi^S \geq 1$ (**T**); $\xi^I \geq 1$ (**T**); $\xi^i \geq 1$ (**T**) (31)

Internal forces:

$$n = \eta - \gamma(\eta - 1), \qquad m = (1-\gamma)\mu. \tag{32}$$

Stiffness matrix components:

$$h_{11} = h_{22} = 1 - \gamma, \qquad h_{12} = h_{21} = 0. \tag{33}$$

Domain ⑤ (Fig. 12): $-1 \leq \xi^s \leq 1$ (**E**); $\xi^S > 1$ (**T**); $\xi^I > 1$ (**T**); $\xi^i > 1$ (**T**) (34)

Internal forces:

$$n = \frac{1}{1+k_A}\left(\eta - \frac{\gamma}{4\mu}(\mu+\eta-1)^2 + k_A(\eta - \gamma(\eta - 1))\right). \tag{35}$$

$$m = \frac{1}{1+k_I}\left(\mu - \frac{\gamma}{4\mu^2}(\mu+\eta-1)^2(2\mu-\eta+1) + k_I(1-\gamma)\mu\right). \tag{36}$$

Stiffness matrix components:

$$h_{11} = \frac{1}{1+k_A}\left(1-\frac{\gamma}{2\mu}(\mu+\eta-1)+k_A(1-\gamma)\right), \tag{37a}$$

$$h_{12} = -\frac{\gamma}{1+k_A}\frac{1}{4\mu^2}(\mu+\eta-1)(\mu-\eta+1), \tag{37b}$$

$$h_{21} = -\frac{\gamma}{1+k_I}\frac{3}{4\mu^2}(\mu+\eta-1)(\mu-\eta+1), \tag{37c}$$

$$h_{22} = \frac{1}{1+k_I}\left(1-\frac{\gamma}{2\mu}(\mu+\eta-1)\left(1-\frac{(\eta-1)(\mu-\eta+1)}{\mu^2}\right)+k_I(1-\gamma)\right). \tag{37d}$$

Domain ⑥ (Fig. 13): $\xi^s < -1$ (**C**); $\xi^S > 1$ (**T**); $\xi^I > 1$ (**T**); $\xi^i > 1$ (**T**) (38)

Internal forces:

$$n = \frac{1}{1+k_A}\left(\eta-\gamma\frac{\eta}{\mu}(\mu-1)+k_A(\eta-\gamma(\eta-1))\right). \tag{39}$$

$$m = \frac{1}{1+k_I}\left(\mu-\gamma\left(\mu-\frac{3}{2}+\frac{3\eta^2+1}{2\mu^2}\right)+k_I(1-\gamma)\mu\right). \tag{40}$$

Stiffness matrix components:

$$h_{11} = \frac{1}{1+k_A}\left(1-\frac{\gamma}{\mu}(\mu-1)+k_A(1-\gamma)\right), \tag{41a}$$

$$h_{12} = -\frac{\gamma}{1+k_A}\frac{\eta}{\mu^2}, \tag{41b}$$

$$h_{21} = -\frac{\gamma}{1+k_I}\frac{3\eta}{\mu^2}, \tag{41c}$$

$$h_{22} = \frac{1}{1+k_I}\left(1-\gamma\left(1-\frac{3\eta^2+1}{\mu^3}\right)+k_I(1-\gamma)\right). \tag{41d}$$

Domain ⑦ (Fig. 14): $-1 \le \xi^s \le 1$ (**E**); $-1 \le \xi^S \le 1$ (**E**); $\xi^I > 1$ (**T**); $\xi^i > 1$ (**T**) (42)

Internal forces:

$$n = \frac{1}{1+k_A}\left(\eta - \frac{\gamma}{4\mu}\left(\mu+\eta-1\right)^2 + k_A\left(\eta - \frac{\gamma}{4\alpha_h\mu}\left(\alpha_h\mu+\eta-1\right)^2\right)\right). \tag{43}$$

$$m = \frac{1}{1+k_I}\left(\mu - \frac{\gamma}{4\mu^2}\left(\mu+\eta-1\right)^2\left(2\mu-\eta+1\right)+\ldots \right.$$
$$\left. \ldots+\frac{k_I}{\alpha_h}\left(\alpha_h\mu - \frac{\gamma}{4\alpha_h{}^2\mu^2}\left(\alpha_h\mu+\eta-1\right)^2\left(2\alpha_h\mu-\eta+1\right)\right)\right). \tag{44}$$

Stiffness matrix components:

$$h_{11} = \frac{1}{1+k_A}\left(1 - \frac{\gamma}{2\mu}\left(\mu+\eta-1\right) + k_A\left(1 - \frac{\gamma}{2\alpha_h\mu}\left(\alpha_h\mu+\eta-1\right)\right)\right), \tag{45a}$$

$$h_{12} = -\frac{\gamma}{1+k_A}\left(\frac{1}{4\mu^2}\left(\mu+\eta-1\right)\left(\mu-\eta+1\right)+\ldots \right.$$
$$\left. \ldots+\alpha_h\, k_A\left(\frac{1}{4\alpha_h{}^2\mu^2}\left(\alpha_h\mu+\eta-1\right)\left(\alpha_h\mu-\eta+1\right)\right)\right), \tag{45b}$$

$$h_{21} = -\frac{\gamma}{1+k_I}\left(\frac{3}{4\mu^2}\left(\mu+\eta-1\right)\left(\mu-\eta+1\right)+\ldots \right.$$
$$\left. \ldots+\frac{k_I}{\alpha_h}\left(\frac{3}{4\alpha_h{}^2\mu^2}\left(\alpha_h\mu+\eta-1\right)\left(\alpha_h\mu-\eta+1\right)\right)\right), \tag{45c}$$

$$h_{22} = \frac{1}{1+k_I}\left(1 - \frac{\gamma}{2\mu}\left(\mu+\eta-1\right)\left(1 - \frac{\left(\eta-1\right)\left(\mu-\eta+1\right)}{\mu^2}\right)+\ldots \right.$$
$$\left. \ldots+k_I\left(1 - \frac{\gamma}{2\alpha_h\mu}\left(\alpha_h\mu+\eta-1\right)\left(1 - \frac{\left(\eta-1\right)\left(\alpha_h\mu-\eta+1\right)}{\alpha_h{}^2\mu^2}\right)\right)\right). \tag{45d}$$

Domain ⑧ (Fig. 15): $\xi^s < -1$ (**C**); $-1 \le \xi^S \le 1$ (**E**); $\xi^I > 1$ (**T**); $\xi^i > 1$ (**T**) (46)

Internal forces:

$$n = \frac{1}{1+k_A}\left(\eta - \gamma\,\frac{\eta}{\mu}(\mu-1) + k_A\left(\eta - \frac{\gamma}{4\alpha_h\mu}(\alpha_h\mu+\eta-1)^2\right)\right). \tag{47}$$

$$m = \frac{1}{1+k_I}\left(\mu - \gamma\left(\mu - \frac{3}{2} + \frac{3\eta^2+1}{2\mu^2}\right) + \ldots \right.$$
$$\left. \ldots + \frac{k_I}{\alpha_h}\left(\alpha_h\mu - \frac{\gamma}{4{\alpha_h}^2\mu^2}(\alpha_h\mu+\eta-1)^2(2\alpha_h\mu-\eta+1)\right)\right). \tag{48}$$

Stiffness matrix components:

$$h_{11} = \frac{1}{1+k_A}\left(1 - \frac{\gamma}{\mu}(\mu-1) + k_A\left(1 - \frac{\gamma}{2\alpha_h\mu}(\alpha_h\mu+\eta-1)\right)\right), \tag{49a}$$

$$h_{12} = -\frac{\gamma}{1+k_A}\left(\frac{\eta}{\mu^2} + \alpha_h\,k_A\left(\frac{1}{4{\alpha_h}^2\mu^2}(\alpha_h\mu+\eta-1)(\alpha_h\mu-\eta+1)\right)\right), \tag{49b}$$

$$h_{21} = -\frac{\gamma}{1+k_I}\left(\frac{3\eta}{\mu^2} + \frac{k_I}{\alpha_h}\left(\frac{3}{4{\alpha_h}^2\mu^2}(\alpha_h\mu+\eta-1)(\alpha_h\mu-\eta+1)\right)\right), \tag{49c}$$

$$h_{22} = \frac{1}{1+k_I}\left(1 - \gamma\left(1 - \frac{3\eta^2+1}{\mu^3}\right) + \ldots \right.$$
$$\left. \ldots + k_I\left(1 - \frac{\gamma}{2\alpha_h\mu}(\alpha_h\mu+\eta-1)\left(1 - \frac{(\eta-1)(\alpha_h\mu-\eta+1)}{{\alpha_h}^2\mu^2}\right)\right)\right). \tag{49d}$$

Domain ⑨ (Fig. 16): $\xi^s < -1$ (**C**); $\xi^S \le -1$ (**C**); $\xi^I > 1$ (**T**); $\xi^i > 1$ (**T**) (50)

Internal forces:

$$n = \frac{1}{1+k_A}\left(\eta - \gamma\,\frac{\eta}{\mu}(\mu - 1) + k_A\left(\eta - \gamma\,\frac{\eta}{\alpha_h\mu}(\alpha_h\mu - 1)\right)\right). \tag{51}$$

$$m = \frac{1}{1+k_I}\left(\mu - \gamma\left(\mu - \frac{3}{2} + \frac{3\eta^2+1}{2\mu^2}\right) + \frac{k_I}{\alpha_h}\left(\alpha_h\mu - \gamma\left(\alpha_h\mu - \frac{3}{2} + \frac{3\eta^2+1}{2\alpha_h{}^2\mu^2}\right)\right)\right). \tag{52}$$

Stiffness matrix components:

$$h_{11} = \frac{1}{1+k_A}\left(1 - \frac{\gamma}{\mu}(\mu - 1) + k_A\left(1 - \frac{\gamma}{\alpha_h\mu}(\alpha_h\mu - 1)\right)\right), \tag{53a}$$

$$h_{12} = -\frac{1}{1+k_A}\left(1 + \frac{k_A}{\alpha_h}\right)\frac{\gamma\eta}{\mu^2}, \tag{53b}$$

$$h_{21} = -\frac{1}{1+k_I}\left(1 + \frac{k_I}{\alpha_h{}^3}\right)\frac{3\gamma\eta}{\mu^2}, \tag{53c}$$

$$h_{22} = \frac{1}{1+k_I}\left(1 - \gamma\left(1 - \frac{3\eta^2+1}{\mu^3}\right) + k_I\left(1 - \gamma\left(1 - \frac{3\eta^2+1}{\alpha_h{}^3\mu^3}\right)\right)\right). \tag{53d}$$

# 4. Comparison with classical numerical methods

## *4.1. Interest of this analytical approach*

First of all, it should be emphasised that this analytical model has been developed in order to be integrated in a computer program for non linear analysis of steel structures.

Generally, this kind of software is based on the displacement method. Using the compatibility conditions between the cinematic variables of the problem, it is possible to calculate the section deformations after the structure displacements.

To evaluate the yielding spreading in a cross-section by means of classical numerical methods, it is necessary to mesh each cross-section into several elementary layers or fibres. The precision of the results and, consequently, the good convergence of the non linear procedure, depend on the mesh refinement which, on the other hand, may lead to very heavy calculations.

The average strain $\varepsilon$ in each fibre or layer need to be determined from the global deformations $\varepsilon_N$ and $\chi$. Then, the average stress $\sigma$ and the stiffness ratios must be calculated using the material constitutive law. Finally, the internal forces and stiffness matrix components should be obtained in the whole section by numerical integration of the stresses and stiffness ratios along the whole cross-sections.

This is a very heavy and long process when great deals of cross-sections need to be analysed, since a large number of deformed states need to be calculated along the non linear behaviour of the structure.

Using the proposed analytical model, the numerical integration procedure is no longer required since it is based on relationships that have been established after a former analytical integration. So, only simple calculations are needed to determine the cross-section internal loads and stiffness matrix components after its global deformation values.

### *4.2. Use of the reduced variables*

The main interest to use reduced variables lies on the separation of the physical phenomena from the numerical quantification of the model variables associated to a specified system of units.

The reduced variables result from the division of these model variables by suitable "scale factors", and their variations depend on "behaviour factors", which control the evolution of the cross-section in the elastic and elastic-plastic domains. In order to clarify the meaning of these factors, let us consider the following example:

An American wide flange beam W610×230×113, according to the ASTM A6-05 standard, is submitted to an axial force $N$ = 2537.5 kN and to a bending moment $M$ = 216.04 kN.m. The cross-section area of this shape is $A$ = 14500 mm$^2$ and its elastic section modulus is $W_{el}$ = 2881×10$^3$ mm$^3$. The yield strength of the constitutive material is $\sigma_y$ = 250 N/mm$^2$.

These values may be meaningless for those who are not familiar with the SI Unit System. In USA, for example, the values of the same variables would be $N$ = 570.45 kip, $M$ = 159.35 kip.ft, $A$ = 22.475 in$^2$, $W_{el}$ = 175.8 8 in$^3$ and $\sigma_y$ = 36.3 ksi. These numerical values are rather different from the previous ones, that means that the perception of their physical meaning will be totally different, depending on the Unit System applied.

If the internal forces are expressed in reduced variables, according to Eqs. (5)-(6), the obtained values are:

- with the SI units:

$$n = N/N_y = N/\left(EA\varepsilon_y\right) = N/\left(A\sigma_y\right) = 2537500/\left(14500\times 250\right) = 0.7$$

$$m = M/M_y = M/\left(EI\,\varepsilon_y/v_M\right) = M/\left(W_{el}\sigma_y\right) = 216.04\times 10^6/\left(2881\times 10^3\times 250\right) = 0.3$$

- with the American units:

$$n = N/N_y = N/\left(EA\varepsilon_y\right) = N/\left(A\sigma_y\right) = 570450/\left(22.475\times 36300\right) = 0.7$$

$$m = M/M_y = M/\left(EI\,\varepsilon_y/v_M\right) = M/\left(W_{el}\sigma_y\right) = 159350\times 12/\left(175.8\times 36300\right) = 0.3$$

These results show that the values of the reduced variables allow a common understanding to all users whatever the unit system is.

Furthermore, the physical meaning of these variables is more explicit than in the case of dimensional variables. For instance, if a European engineer knows that the axial force in a W610×230×113 profile is $N = 2537.5$ kN, this value is not significant for him if he is not familiar with the characteristics of American wide flange beams.

On the other hand, if he knows that the reduced value is $n = 0.7$, he understands immediately that the cross section is submitted to an axial force equal to 70% of its yielding load $N_y$, under pure axial loading.

Moreover, the values of the reduced internal forces may give some additional physical information. If Eqs. (21) and (4) are used, it is easy to conclude that the reduced strain in the lower fibre is $\xi^i = 0.7+0.3 = 1.0$, which means that the stress in this fibre is equal to $\sigma_y$ and, therefore, the cross-section is at its elastic limit state. The reduced strain at the upper fibre is $\xi^i = 0.7 - 0.3 = 0.4$, which means that the corresponding stress is equal to 40% of the yield strength, $\sigma_y$.

The $N_y$ factor, as well as the $M_y$ factor representing the largest moment in simple bending when the elastic limit of the cross-section is reached, are two examples of the "scale factors" mentioned above. It should be noted that scale factors may be evaluated after the values of other factors. The values of $N_y$ and $M_y$, for example, may be obtained from those of $\sigma_y$, $A$ and $W_{el}$, which, on their turn, may be obtained from the values of $E$ and $\varepsilon_y$, and from the cross-section dimensions $b'$, $b''$, $h'$ and $h''$ (Fig. 7).

In the elastic domain, the relationship between the reduced cross-section global deformations and the internal forces or stiffness matrix components is brought down to

its simplest form, as shown in Eqs. (20)-(21), due to the constant linear relationship given by Hooke's law, $\sigma = E\varepsilon$, which may be also be written under the following reduced form, $\zeta = \xi$.

On the other hand, this linear ratio is no longer valid for the whole cross-section in the elastic-plastic domains, and the relations between the internal forces or stiffness matrix components and the cross-section global deformations depend on "behaviour factors", which reflect the effects of the cross-section geometrical and physical discontinuities on its non linear behaviour.

In this model, the main behaviour factors related to the cross-section geometry are the variables $\alpha_b$ and $\alpha_h$, Eqs. (10) and (11), which are related to the width to thickness ratio of the cross section web and flanges. The other geometrical behaviour factors are the variables $k_A$ and $k_I$, which may be evaluated after the values of $\alpha_b$ and $\alpha_h$. The behaviour factor related to the non linear response of the material is the variable $\gamma$, which relates the tangent modulus of the material in the plastic domain, $E_t$, with the Young's modulus $E$ in the elastic domain, Eq. (3).

### *4.3. Example of calculation for cross-section elastic-plastic behaviour*

This example aims to demonstrate the simplicity of application of the proposed analytical formulation. It concerns a HEB 220 cross-section bent about its strong axis, whose geometrical characteristics and reduced parameters $\alpha_b$ and $\alpha_h$ are:

$h = 220$ mm, $b = 220$ mm, $t_f = 16$ mm, $t_w = 9.5$ mm, $A = 9104$ mm$^2$,

$I_y = 8091 \times 10^4$ mm$^4$, $\alpha_b$ =0.9560, $\alpha_h$=0.8492, $k_A = -0.8119$ and $k_I = -0.5855$. It is made from S235 steel grade with $E = 210$ kN/mm$^2$, no strain hardening, $E_t = 0$ ($\gamma = 1$),

and $\sigma_y = 235$ N/mm$^2$ (so $\varepsilon_y = 1.12 \times 10^{-3}$). The ultimate strain $\varepsilon_u$ has been chosen equal to $200\,\varepsilon_y = 224 \times 10^{-3}$.

In this example, the reduced global deformations are chosen equal to $\eta = -0.02$ and $\mu = 1.05$. As mentioned before, the calculations will be carried out with the absolute values of these variables. According to Eq. (**4**), it comes: $\xi^s = 1.03$; $\xi^S = 0.8717$; $\xi^I = 0.9117$; $\xi^i = 1.07$.

According to Eq. (27), the cross-section is within domain ③. Therefore, the reduced internal forces will be evaluated using Eqs. (28)-(29). The corresponding dimensional values are obtained by multiplying the reduced variables by the relevant scale factors.

$$n = \frac{1}{1 - 0.8119}\left(0.02 - \frac{0.02}{1.05}(1.05 - 1) - 0.8119 \times 0.02\right) = 0.01494,$$

and: $N = n\ N_y = n\ E\ A\ \varepsilon_y = 0.01494 \times 210000 \times 9104 \times 1.12 \times 10^{-3} = 31.96$ kN.

$$m = \frac{1}{1 - 0.5855}\left(1.05 - \left(1.05 - \frac{3}{2} + \frac{3 \times 0.02^2 + 1}{2 \times 1.05^2}\right) - 0.5855 \times 1.05\right) = 1.040,$$

and: $M = m\ M_y = m\ E\ I_y \dfrac{\varepsilon_y}{z_M} = 1.040 \times 210000 \times 8091 \times 10^4 \times \dfrac{1.12 \times 10^{-3}}{110} = 179.8$ kN.m.

The axial deformation $\eta$ being negative, the real value of the axial force is $N = -31.96$ kN. This example shows the simplicity of the calculations in the elastic-plastic domains, which allows the needs for memory and computation time to be considerably reduced when compared to those of classical numerical integration processes with fibres or layers models.

The evaluation of the stiffness matrix components may be carried out following the same procedure using Eqs. (30). Nevertheless, it must be emphasised that, if the curvature has a different sign from the one of the axial deformation, the signs of the stiffness components $H_{12}$ and $H_{21}$ have to be changed.

# 5. Use of internal forces as basic variables

## *5.1. Application to a classical cross-section check*

As mentioned before, this analytical model has been developed to be used as a subroutine in a computer program, based on the finite element technique, for the non-linear analysis of steel structures [3]. Its formulation uses the displacements method, the cross-sections internal loads and stiffness matrix components being evaluated as a function of the global deformations ($\eta$ and $\mu$) compatible to the displacements applied to the structure. Since $\eta$ and $\mu$ are the basic variables, it is not always possible to make a direct use of the model analytical expressions in the verification of the cross-section safety to a combination of internal loads (axial force $n$ and bending moment $m$) in the elastic-plastic-domain.

Nevertheless, although the verification of the cross-sections was not the aim of this analytical model, it may still be used in two different ways. The one used here consists in the resolution of the previous analytical relationships as a function of the variables to be calculated. The other one is based on a numerical resolution of the same equations by an iteration procedure [1].

### *5.2. Example of application*

This example concerns the same HEB 220 cross-section described in section 4.2 made, in this case, of a S275 steel grade with $E = 210\,\text{kN/mm}^2$, $E_t = 850\ \text{N/mm}^2$ ($\gamma = 0.9959$), $\sigma_y = 275\ \text{N/mm}^2$ (so $\varepsilon_y = 1.31\times10^{-3}$). The ultimate strain $\varepsilon_u$ has been chosen equal to $200\times10^{-3}$, which means that $\xi_u = 152.7$.

This section is submitted to an axial force $N = \text{-}2500\ \text{kN}$ and a bending moment $M = 14\,\text{kN.m}$. The corresponding reduced values according to Eqs. (5)-(6) are $n = 0.9986$ and $m = 0.0692$.

According to Eq. (20), the cross-section is in its elastic domain if $|\eta| + |\mu| \le 1$. In this case, $\eta = n$, Eq. (21), and $\mu = m$, Eq. (22). So, the cross-section remains elastic when the condition $|n| + |m| \le 1$ is respected.

In this case, $|n| + |m| = 1.0678 > 1$, so the section is no longer in its elastic domain. It may be noted that the cross-section would be able to bear these internal forces in the elastic domain if its yield stress would be greater than $1.0678\times\sigma_y = 294\ \text{N/mm}^2$, which would be the case if it was made of a S355 steel grade ($\sigma_y = 355\ \text{N/mm}^2$).

As the cross-section is not in the elastic domain, it is necessary to find the elastic-plastic domain $\Omega$ where it lies. This search is quite easy when the reduced global deformations ($\eta$ and $\mu$) are known, by using the equations that define the frontiers between the $\Omega$ domains (Eqs. (23), (27), (31), etc.). In this case, only the internal forces are known, so the reduced values of the deformations are needed before the check of the $\Omega$ domains.

The easiest situation is the one where the whole cross-section is totally yielded, under the predominant action of an axial load (domain ④). This situation exists when $\xi^s \geq 1$ which means that $|\eta| - |\mu| \geq 1$, Eq. (31). According to Eq. (32), this condition may also be written under the form $|\eta| - |\mu| = (|n| - \gamma) - |m| \geq 1 - \gamma$, which may also be written as $|n| - |m| \geq 1$.

In this case, $|n| - |m| = 0.9293 < 1$, so the section is not in the domain ④. It may also be noted that the cross-section would be in the domain ④ if its yield stress would be smaller than $0.9293 \times \sigma_y = 255$ N/mm$^2$, which would be the case if it was made of a S235 steel grade ($\sigma_y = 235$ N/mm$^2$).

Nevertheless, the value of $|n| - |m| = 0.9293$ is quite close to 1 which means that the cross section is probably in a domain $\Omega$ close to the domain ④. The closest one is the domain ⑤ (Fig. 6), so this domain is the next one to be checked.

If the values of $n = 0.9986$, $m = 0.0692$, $\gamma = 0.9959$, $k_A = -0.8119$ and $k_I = -0.5855$ are introduced in Eqs. (35)-(36), a system of two equations is obtained where the variables are $\eta$ and $\mu$. The solving of this system gives three set of solutions for these variables:

$\eta = 1.0000106$ and $\mu = 1.0228 \times 10^{-7}$,

$\eta = 8.07216$ and $\mu = 6.68139$,

$\eta = 7.89626$ and $\mu = 7.29984$.

If any of these solutions is within the domain ⑤, it should verify the conditions stated by Eq. (34). The first of these conditions is $-1 \le \xi^S \le 1$, or $-1 \le \eta - \mu \le 1$. Solution a) does not respect this condition since $\eta - \mu = 1.0000105 > 1$. Solution b) gives $\eta - \mu = 1.39077 > 1$ which does not respect the same condition. So, these two solutions are not valid since they have been calculated by Eqs. (35)-(36), which are applicable only in the domain ⑤, and these solutions are not within this domain.

On the other hand, in the case of solution c), the above condition is respected ($\eta - \mu = 0.59641 < 1$). Still, the other three conditions from Eq. (34) need also to be verified. The second condition, $\xi^S = \eta - \alpha_h \mu = 1.697 > 1$, is also verified meaning that this solution is in the domain ⑤ or in the domain ⑥ (Fig. 6). In this case, the third condition ($\xi^I = \eta + \alpha_h \mu > 1$) needs not to be checked since it is always verified when the second condition is respected.

The forth condition $\xi^i = \eta + \mu = 15.196 > 1$ is also verified which means that this solution c) is in the domain ⑤ and not in the domain ⑥ (Fig. 6). Since the four conditions from Eq. (34) are satisfied, it is sure that the correct solution has been found and the cross-section is within the domain ⑤. If not, it would have been necessary to repeat the same process for each one of the other domains until the correct solution is found. This process may appear rather complicated but it may be easily accomplished by the use of a spreadsheet, for instance.

The correct sign of the deformations must now be chosen. Since the axial force is negative, the correct value of the reduced axial deformation will be $\eta = -7.8963$; as the bending moment is positive, the curvature is in fact $\mu = 7.2998$.

Finally, it is necessary to check if the material of the cross-section is able to stand these internal forces and deformations without failure. The absolute value of the maximum strain in the material is $|\eta| + |\mu| = 15.1961$. Since this value is smaller than the ultimate reduced strain of the material $\xi_u = 152.7$, the cross-section did not reach this ultimate state and the cross-section is able to support the given internal loads and the corresponding deformations.

It should be emphasised that these calculations have been carried out considering the influence of strain hardening of the material. If no strain hardening is considered, the cross-section will not be able to bear the given internal loads.

In this case, only a higher steel grade would allow the same cross-section to reach the required resistance. If for instance a S355 steel grade is used, the new reduced values of the internal forces are $n = 0.7735$ and $m = 0.0536$ leading the cross-section to be in the elastic domain ①. The reduced deformations are then $\eta = 0.7735$ and $\mu = 0.0536$.

## 6. Conclusions

The formulation of an analytical elastic-plastic mechanical model is presented in this paper to study steel cross sections bent about their main axes (strong or weak axis).

At first, the basic principles of the formulation are presented; they are based on the analysis of the cross-section global deformations. Then, the application to industrial shapes is explained.

Next, the formulation of the analytical model is presented in detail, allowing internal forces and stiffness matrix components to be evaluated after the global

deformations. The domains of application of the analytical expressions, corresponding to different yielding states of the section, are clearly put in evidence.

Some examples of calculations are provided for traditional hot-rolled sections. The first example emphasises the simplicity of the application of this model in its basic configuration (when the basic variables are the global deformations of the cross-section). The other examples show that this model may also be used to evaluate the behaviour of a cross-section as a function of the internal forces in the elastic and elastic-plastic domains.

This model allows the progressive yielding spreading in the cross-sections to be taken into account. It also integrates the effects of strain hardening on the resistance of cross-sections in the elastic-plastic domain, as well as the restrictions due to the maximum deformation capacity of the material.

It constitutes an efficient, simple and accurate alternative to the numerical models requiring numerical integration over the cross-section meshed into elementary fibres or layers.

## References

[1] Baptista, A.M., Muzeau, J.P. Formulation analytique pour le calcul élastoplastique de sections en I ou en H fléchies autour de l'axe fort. *Construction Métallique*, **4**, 2001, 31-57.

[2] Baptista, A.M. Modèle non linéaire géométrique et matériel fondé sur l'analyse des déformations globales des sections – *PhD Thesis, Blaise Pascal University,* Clermont-Ferrand, November 1994.

[3] Baptista, A.M., Muzeau, J.P. Modèle analytique en déformations globales pour l'étude élastique non linéaire de sections industrielles. *Construction Métallique*, **4**, 1996, 29-40.

[4] Baptista, A.M., Muzeau, J.P. Analytical model for non-linear analysis of steel cross-sections. *International Conference "New Technologies in Structural Engineering", NEW TECH'97, IABSE-FIP*, Lisbon, Portugal, July 1997, 1061-1068.

[5] CEN/TC 250. Eurocode 3: Design of steel structures - Part 1-1: General rules and rules for buildings. *European Standard* EN 1993-1-1:2005.

# Figure captions

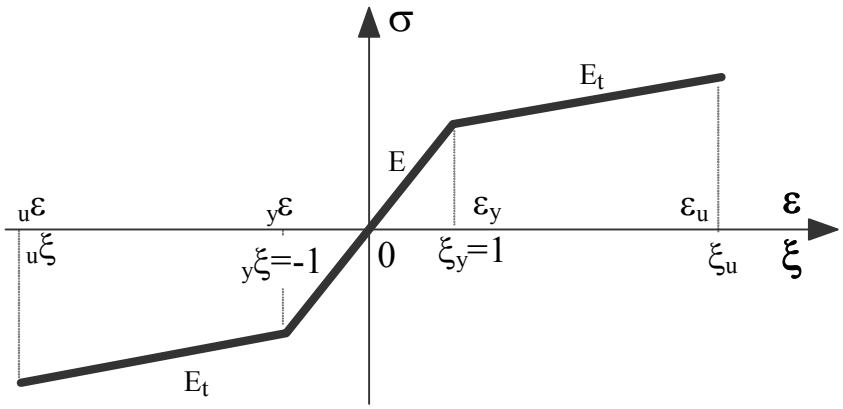


**Figure 1 - Material constitutive law**

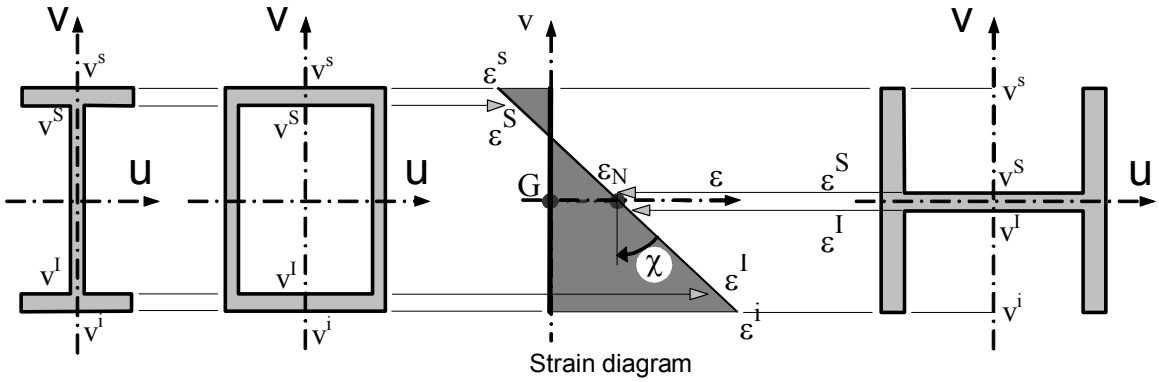


**Figure 2 - Definition of strains for different types of cross-sections**

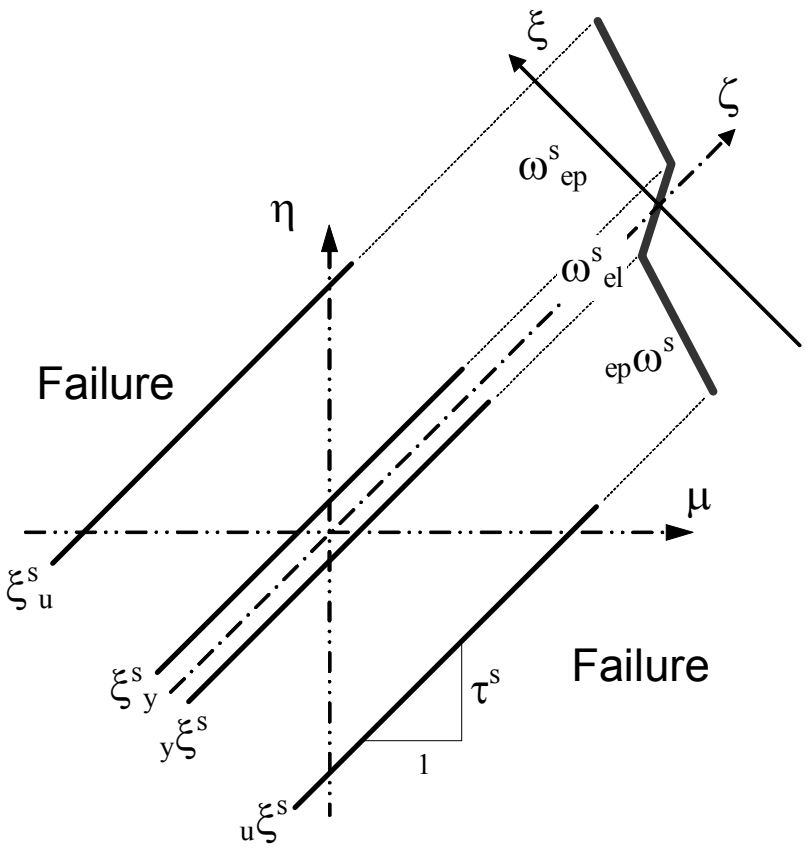


**Figure 3 - Deformation domains ω of the cross-section upper fibre**

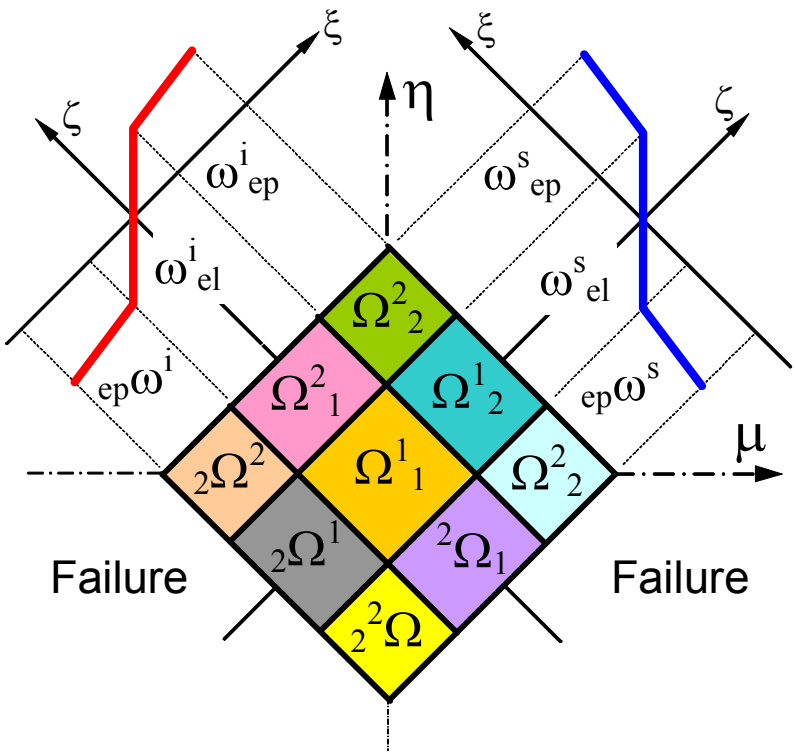


**Figure 4 - Domains of evolution of the global deformations in a rectangular cross-section**

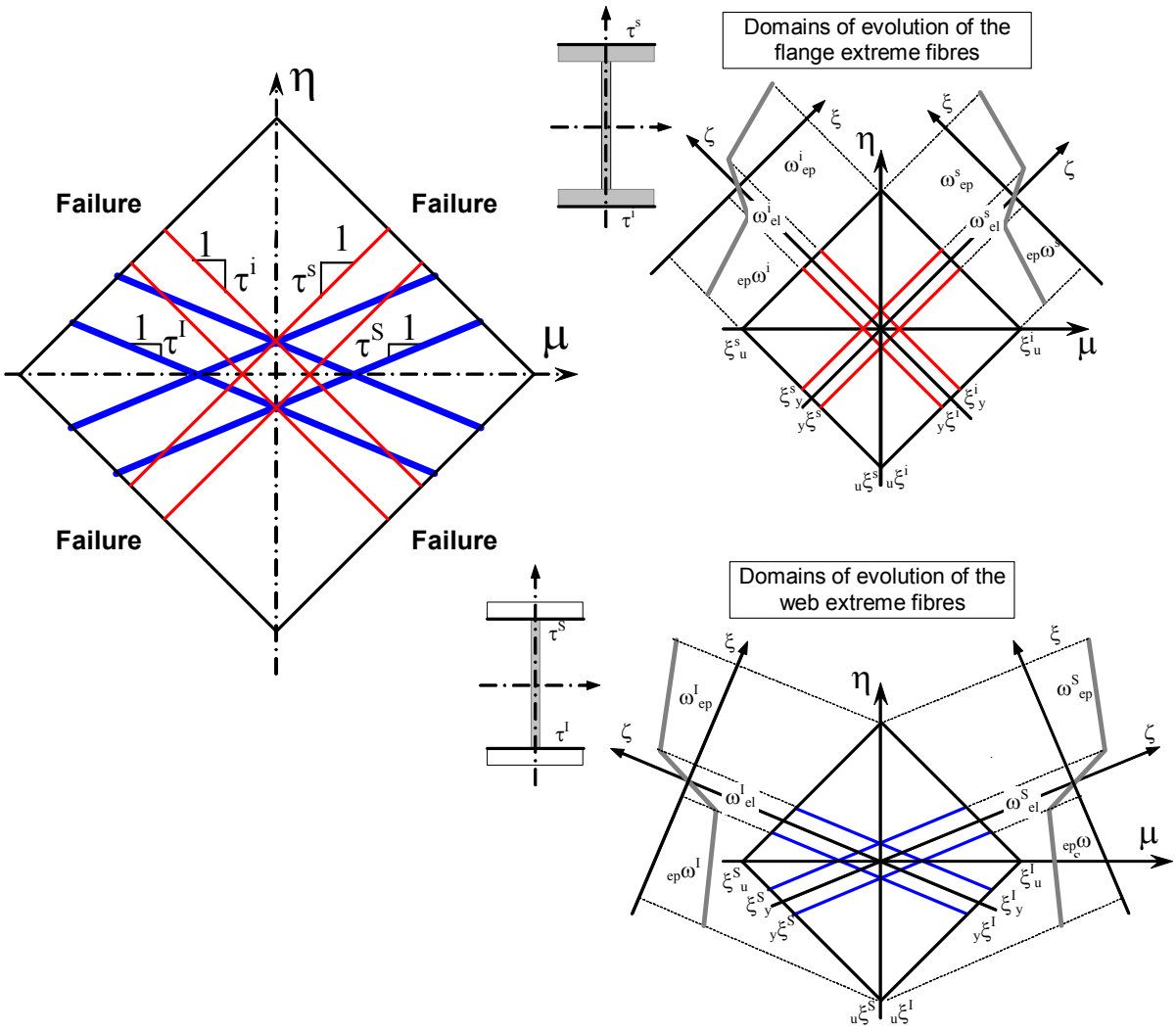


**Figure 5 - Domains of evolution of the global deformations in an I-shape**

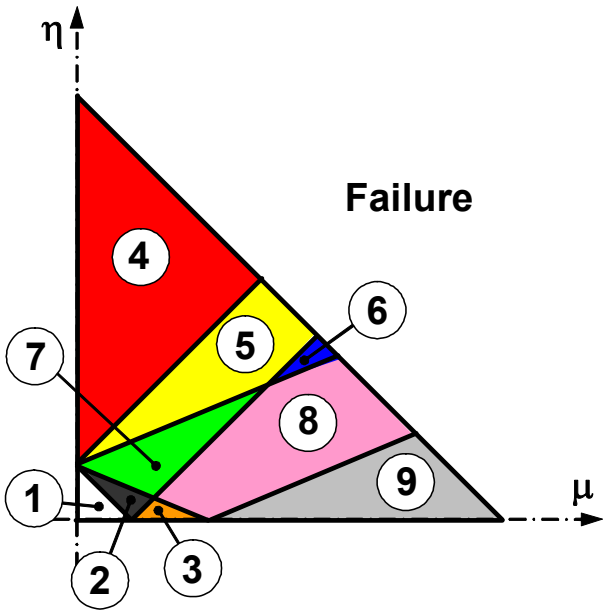


**Figure 6 - Domains in the first quadrant of the global deformations for an I-shape**

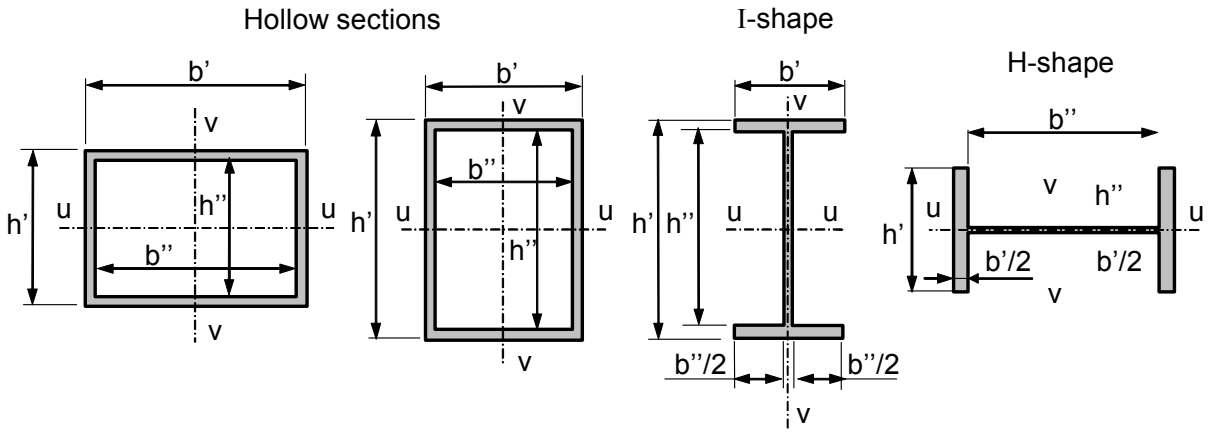


**Figure 7 - Main dimensions of I-shapes and rectangular hollow sections**

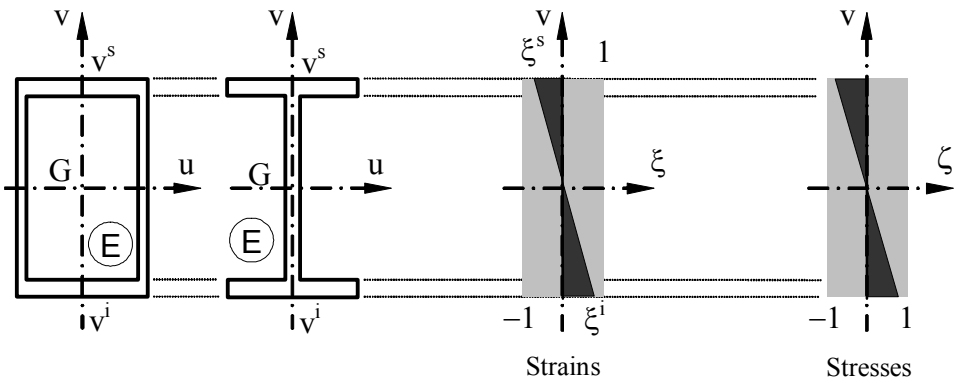


**Figure 8 - Strain and stress diagrams in domain ①.**

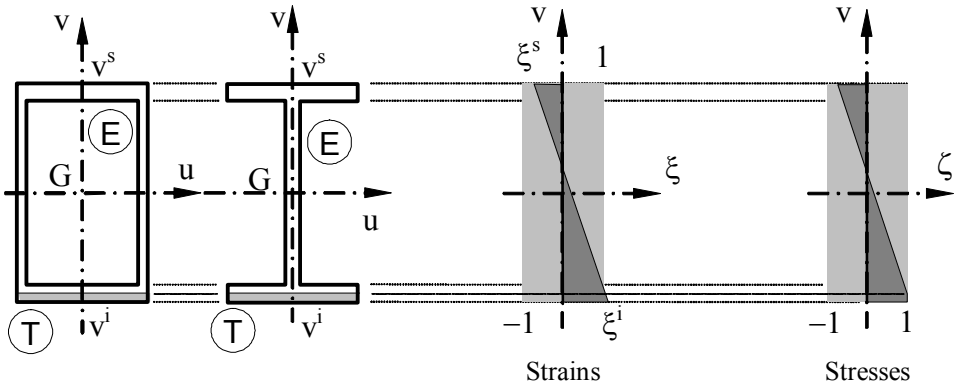


**Figure 9 - Strain and stress diagrams in domain ②**

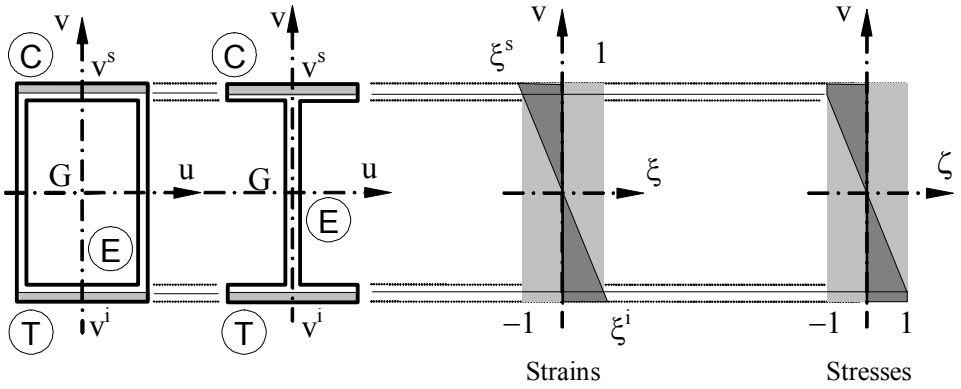


**Figure 10 - Strain and stress diagrams in domain ③**

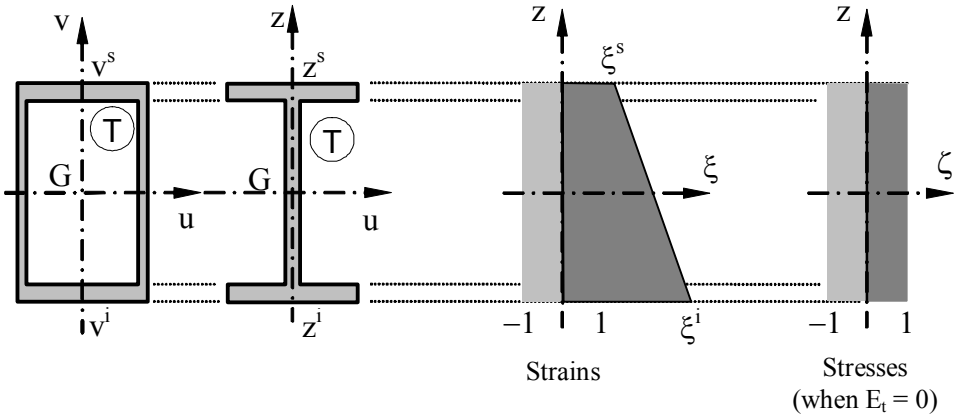


**Figure 11 - Strain and stress diagrams in domain ④**

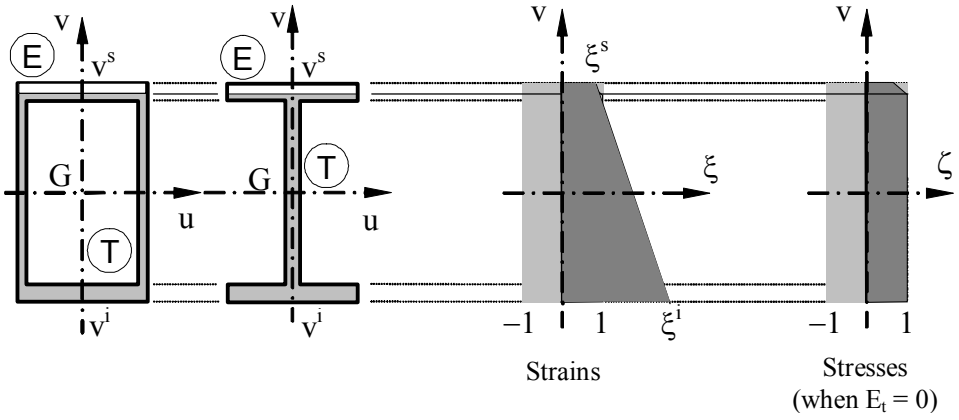


**Figure 12 - Strain and stress diagrams in domain ⑤**

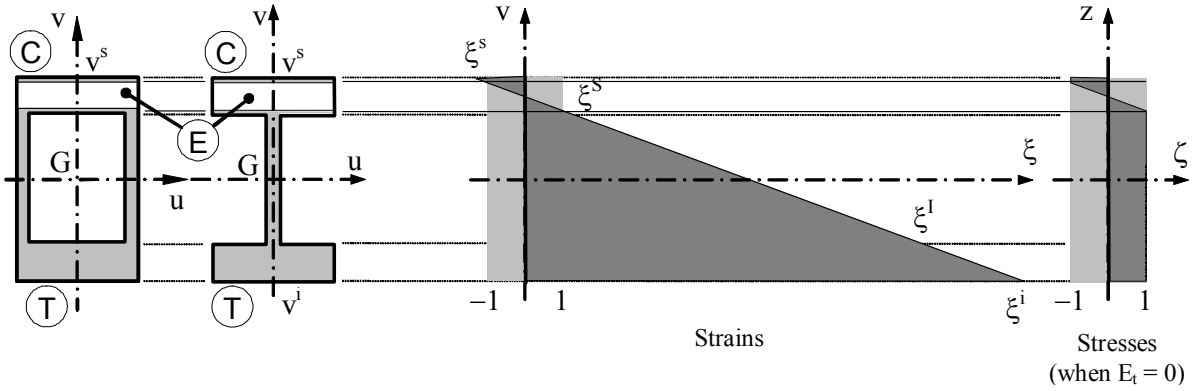


**Figure 13 - Strain and stress diagrams in domain ⑥**

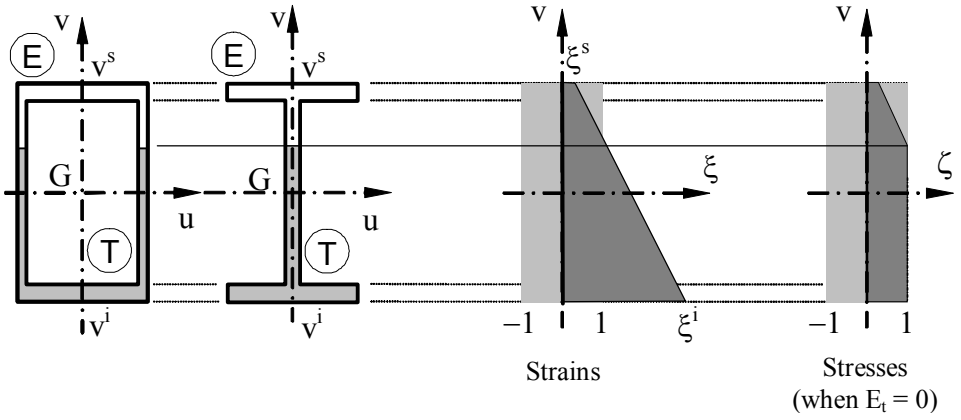


**Figure 14 - Strain and stress diagrams in domain ⑦**

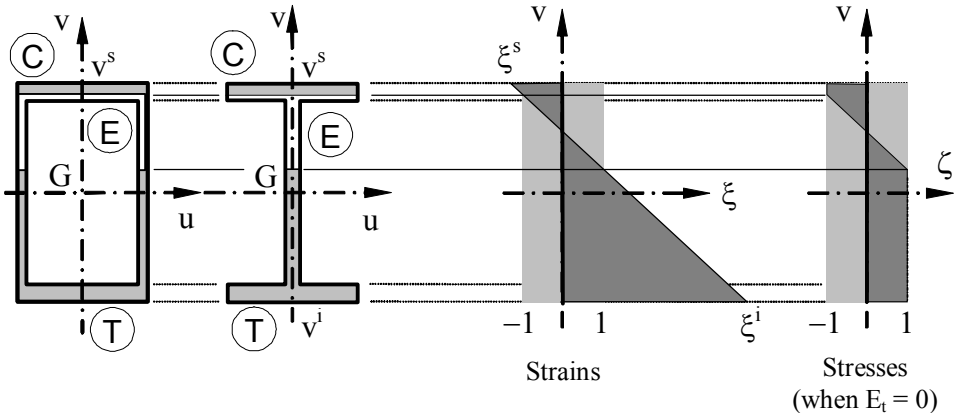


**Figure 15 - Strain and stress diagrams in domain ⑧**

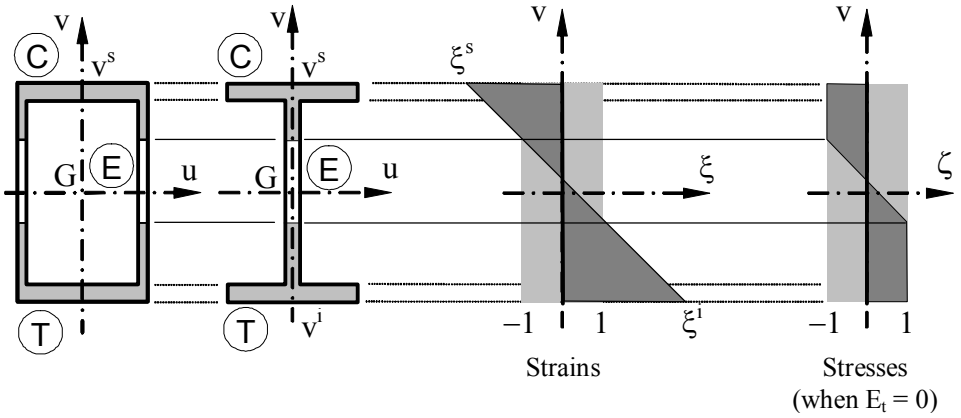


**Figure 16 - Strain and stress diagrams in domain ⑨**